

Available online at [www.sciencedirect.com](http://www.sciencedirect.com)

SciVerse ScienceDirect

journal homepage: [www.elsevier.com/locate/he](http://www.elsevier.com/locate/he)

# Clustering effects on liquid oxygen (LOX) droplet vaporization in hydrogen environments at subcritical and supercritical pressures

Hua Meng<sup>a</sup>, Vigor Yang<sup>b,\*</sup>

<sup>a</sup> School of Aeronautics and Astronautics, Zhejiang University, Hangzhou, Zhejiang 310027, China

<sup>b</sup> Daniel Guggenheim School of Aerospace Engineering, Georgia Institute of Technology, Atlanta, GA 30332, USA

## ARTICLE INFO

### Article history:

Received 8 February 2012

Received in revised form

17 May 2012

Accepted 23 May 2012

Available online 16 June 2012

### Keywords:

Droplet vaporization

Clustering effect

High pressure

Supercritical condition

## ABSTRACT

A droplet-in-bubble approach has been incorporated into a previously developed high-pressure droplet vaporization model to study the clustering effects on a liquid oxygen (LOX) droplet evaporating in hydrogen environments under both sub- and supercritical conditions. A broad range of ambient pressures and temperatures are considered. Results indicate that pressure exerts strong influence on droplet vaporization behaviors in a dense cluster environment. Increasing ambient pressure reduces droplet interactions and significantly decreases the droplet vaporization time. The effect of ambient temperature on droplet interactions is found to be very weak. The present study is intended to illuminate the underlying physics of droplet clustering phenomena in combustion devices.

Copyright © 2012, Hydrogen Energy Publications, LLC. Published by Elsevier Ltd. All rights reserved.

## 1. Introduction

Most liquid-fueled combustion devices involve atomization of injected fuels into small droplets, which then undergo a series of evaporation, mixing, and burning processes. In practical diesel, gas-turbine, and rocket engines, such processes often occur at high pressures either near or above the critical states of the fuels. Droplet behaviors at high pressures are thus of fundamental importance in achieving improved understandings of combustion physics [1].

Many experimental and numerical studies [2–13] have been carried out to investigate high-pressure droplet vaporization and combustion phenomena in engine operation conditions. Most of these studies focused on a single fuel droplet either evaporating or burning in a quiescent environment. Results revealed many characteristics distinct from

their low-pressure counterparts, due to the unsteady transport phenomena both within and outside the fuel droplet, dissolution of ambient gases into the droplet, thermodynamic non-idealities, and transport anomalies at high pressures [1].

Although much progress has been achieved in studying single droplet vaporization and combustion at high pressures, current available data are insufficient for the accurate modeling of two-phase combustion processes. Experimental observations of spray combustion clearly indicate that droplets normally evaporate in a cluster environment, and behaviors of individual droplets are significantly affected by the surrounding droplets [14,15]. Only limited studies have been conducted so far for clustered droplet vaporization at high pressures. Jiang and Chiang [16] numerically studied n-pentane fuel droplet vaporization in a cluster. A one-dimensional spherically-symmetric high-pressure droplet

\* Corresponding author.

E-mail addresses: [menghua@zju.edu.cn](mailto:menghua@zju.edu.cn) (H. Meng), [vigor.yang@aerospace.gatech.edu](mailto:vigor.yang@aerospace.gatech.edu) (V. Yang).

Nomenclature	
$A$	Control surface area or droplet surface area
$D$	Droplet diameter
$D_{im}$	Effective mass diffusivity
$e_t$	Total internal energy
$\bar{h}_i$	Partial-mass enthalpy of species $i$
$K_{vap,i}$	Vaporization kinetic coefficient
$\dot{m}$	Droplet mass evaporation rate
$\vec{n}$	Normal outward unit surface vector
$p$	Pressure
$q_e$	Thermal diffusion flux
$q_i$	Mass diffusion flux of species $i$
$r$	Spherical coordinate
$R$	Droplet radius
$\dot{R}$	Time variation rate of droplet radius
$R_{bub}$	Bubble radius
$t$	Time
$T$	Temperature
$v$	Velocity
$V$	Control volume
$w$	Control surface velocity
$Y_i$	Mass fraction of species $i$
<i>Greek symbols</i>	
$\lambda$	Thermal conductivity
$\mu$	Chemical potential
$\rho$	Density
$\tau$	Dimensionless droplet lifetime
<i>Subscripts</i>	
bub	bubble
d	droplet
i	species
int	interface
0	initial value
<i>Superscripts</i>	
g	gas phase
l	liquid phase

vaporization model, similar to those in Refs [2,5], was coupled with the sphere-of-influence concept [17] to investigate the clustering effects on the droplet vaporization characteristics. The sphere-of-influence concept assumes that the fuel droplets are uniformly distributed in a spray, and each droplet evaporates in a finite sphere within a droplet cluster, instead of in an infinite space, as for an isolated droplet. Jiang and Chiang [16] concluded that the droplet vaporization time is significantly prolonged due to the droplet clustering effect. Increasing the ambient pressure weakens the droplet interaction considerably. The sphere-of-influence method was also employed by Harstad and Bellan [18] to numerically investigate liquid oxygen (LOX) droplet vaporization and interaction in quiescent hydrogen environments at supercritical pressures. A fluctuation theory, which assumes thermodynamic non-equilibrium at the droplet surface, was implemented for calculating the droplet vaporization rate. Uncertainties, however, remained for determining the kinetic constant in the model, because of the lack of an accurate evaluation method.

Given its practical importance, fundamental research is still needed to elucidate the underlying physics of droplet vaporization in a dense cluster environment, and particularly for the LOX/hydrogen system, which has not been comprehensively investigated. In the present work, a numerical study of the clustering effects on a LOX droplet evaporating in a hydrogen environment is conducted. Both sub- and supercritical conditions are treated. A droplet-in-bubble approach [19], which is suitable for solving droplet vaporization in a dense droplet cluster, is incorporated into a well-established droplet vaporization model [12], which accommodates a self-consistent treatment of high-pressure phenomena, including thermodynamic non-idealities, transport anomalies, and transient behaviors. The effects of the ambient pressure and temperature on the LOX droplet vaporization rate in a dense cluster environment are explored in detail. The Results will

contribute to the two-phase modeling of high-pressure hydrogen/oxygen combustion processes.

## 2. Theoretical formulations and numerical treatment

The physical model of concern is the LOX droplet evaporating inside a dense droplet cluster, as shown schematically in Fig. 1a. Inside the cluster, because of the droplet interaction, mass and energy exchanges around each droplet are isolated. This leads to the droplet-in-bubble concept described in Ref. [19], which assumes that each droplet evaporates in an isolated and slightly elastic spherical space. In the present study, droplets evaporate in a quiescent environment, resulting in a spherically-symmetric configuration shown in Fig. 1b. The edge regions outside droplet bubbles are distributed equally into each bubble. The equivalent radius of a gas bubble is thus calculated based on the volumes of the original bubble and the allocated edge regions, and is slightly larger than half the distance between two droplets.

The droplet-in-bubble approach is incorporated into a well-validated droplet vaporization numerical scheme previously developed for treating droplet vaporization at high pressures [12]. The formulation is based on a complete set of conservation equations of mass, momentum, energy, and chemical species in a spherical coordinate system for both liquid and gaseous phases. Because the velocity is small over the entire flowfield, the momentum equation is simplified to be a constant-pressure condition. Before the droplet reaches the critical mixing state, its surface is clearly defined and can be accurately tracked using a system of moving meshes. The moving boundary problem can be formulated more conveniently using the control-volume method. The conservation equations take the following form:

mass conservation

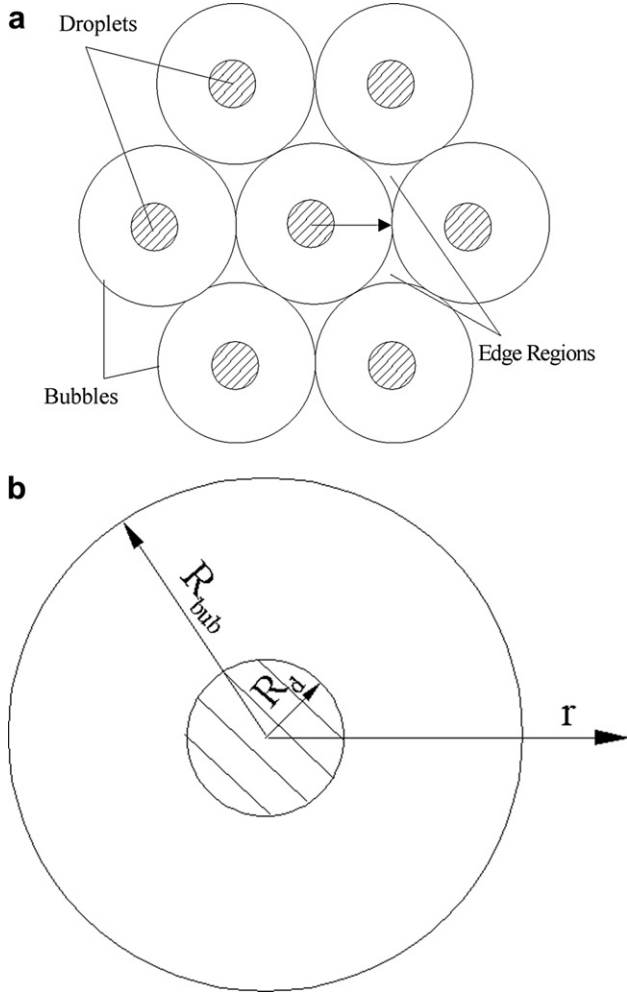


**Fig. 1 – Schematic diagrams of (a) a droplet cluster, and (b) an evaporating droplet in a bubble.**

$$\frac{d}{dt} \int_{V(t)} \rho dV + \int_{A(t)} \rho(\vec{v} - \vec{w}) \cdot \vec{n} dA = 0 \quad (1)$$

momentum conservation

$$\nabla P = 0 \quad (2)$$

energy conservation

$$\begin{aligned} \frac{d}{dt} \int_{V(t)} \rho e_t dV + \int_{A(t)} \rho(\vec{v} - \vec{w}) e_t \cdot \vec{n} dA \\ = - \int_{A(t)} \vec{q}_e \cdot \vec{n} dA - \int_{A(t)} p \vec{v} \cdot \vec{n} dA \end{aligned} \quad (3)$$

species conservation

$$\frac{d}{dt} \int_{V(t)} \rho Y_i dV + \int_{A(t)} \rho Y_i (\vec{v} - \vec{w}) \cdot \vec{n} dA = - \int_{A(t)} \vec{q}_i \cdot \vec{n} dA \quad (4)$$

In the above equations, the variable  $\vec{w}$  denotes the moving velocity of the control surface, which is dictated by the movement of the droplet surface during the vaporization

process. Standard notations in fluid mechanics are used and defined in the Nomenclature.

The energy and species diffusion fluxes take the following forms:

$$\vec{q}_e = -\lambda \nabla T - \sum_i^N \vec{q}_i \bar{h}_i \quad (5)$$

$$\vec{q}_i = -\rho D_{im} \nabla Y_i \quad (6)$$

In these two equations, the Soret and Dufour effects are omitted because of their negligible influence on the vaporization phenomena [12].

Before the droplet reaches its critical mixing state, thermodynamic phase equilibrium prevails at the droplet surface. It can be expressed as

$$T^g = T^l, p^g = p^l, \mu_i^g = \mu_i^l \quad (7)$$

In addition, mass, energy, and species are conserved across this interface.

$$\dot{m} = \rho(\vec{v} - \dot{R}) \cdot \vec{n} A|_{r=R_+} = \rho(\vec{v} - \dot{R}) \cdot \vec{n} A|_{r=R_-} \quad (8a)$$

$$\dot{m}_i = [\dot{m} Y_i + \vec{q}_i \cdot \vec{n} A]_{r=R_+} = [\dot{m} Y_i + \vec{q}_i \cdot \vec{n} A]_{r=R_-} \quad (8b)$$

$$-\lambda \nabla T|_{r=R_-} = -\lambda \nabla T|_{r=R_+} + \sum_{i=1}^N \dot{m}_i (\bar{h}_i^g - \bar{h}_i^l) \quad (8c)$$

Because of the simplification of the momentum equation, the pressure equality at the droplet surface is satisfied automatically. A robust and efficient treatment based on the irreversible thermodynamic theorem is further developed to handle the other thermodynamic equilibrium conditions and the conservation of energy and species across the droplet surface [12]. For example, the following expression is employed for treating the species transport across the interface:

$$\dot{m}_i = K_{vap,i} (\mu_i^l - \mu_i^g) \quad (9)$$

By using a large vaporization kinetic coefficient  $K_{vap,i}$  in this equation, the thermodynamic equilibrium condition for the chemical potential and the species flux conservation at the droplet surface can be closely approached. A similar expression based on temperature differences can be further derived for calculating thermal conduction across the droplet interface and for closely approaching the thermal conditions [12].

Once the critical mixing point is reached, the distinction between the two phases across the droplet surface disappears. Afterwards, a single phase treatment is adopted to determine the subsequent vaporization process at a supercritical state. The droplet surface is defined by the location of the critical mixing temperature [1,12].

An accurate estimation of thermophysical properties over the entire fluid thermodynamic regime is a prerequisite in any numerical study of high-pressure transport phenomena. In our prior work, a general framework was established for property evaluations. An extended corresponding-state method was employed to calculate fluid transport properties, including viscosity and thermal conductivity [1,10]. Fundamental thermodynamics theories and the Soave-

**Table 1 – Critical properties of oxygen and hydrogen.**

	Pressure (atm)	Temperature (K)
H <sub>2</sub>	12.73	33.0
O <sub>2</sub>	49.74	154.6

Redlich-Kwong (SRK) equation of state were employed to determine thermodynamic properties, including heat capacity and internal energy [1,20]. A simple corresponding-state approach was implemented to account for pressure effects on mass diffusivity [1,10]. These property-evaluation schemes were previously employed for studying droplet vaporization under various flow conditions [2,3,5,10,12,13], cryogenic fluid injection, mixing, and combustion at supercritical conditions [21–24], and supercritical heat transfer of hydrocarbon fuels [25–27]. More details concerning this numerical model for studying high-pressure droplet vaporization can be found in Refs. [10,12,20].

In the present numerical study, the following boundary conditions are needed:

at the droplet center

$$\nabla T = 0; \nabla Y_i = 0; \vec{v} = \vec{w} = 0 \quad (10)$$

at the bubble surface

$$\nabla T = 0; \nabla Y_i = 0; \vec{v} = \vec{w} \quad (11)$$

According to Eq. (11), the bubble surface is isolated and elastic, and during the numerical calculations, it decreases slightly. This means that the volume of the dense droplet cluster shrinks slightly due to droplet evaporation. The bubble surface moves with the local fluid velocity, while the other control surfaces move with the droplet surface, thereby resulting in coarse meshes in the gas bubble region. An adaptive grid system is used to refine the grid once it reaches 1.5 times the original value.

### 3. Results and discussion

The theoretical and numerical framework outlined in the preceding section is employed to study the behaviors of a LOX droplet evaporating inside a hydrogen bubble at both sub- and supercritical pressures, as shown in Fig. 1b. The initial temperature of the LOX droplet is 100 K, and its initial diameter is 100  $\mu\text{m}$ . The ambient temperature ranges from 700 K to 1500 K. Three different ambient pressures are considered, including 10 and 30 atm in the subcritical regime and 100 atm at the supercritical condition. The critical properties of oxygen and hydrogen are listed in Table 1. A grid-independence study was performed to verify that a total of 160 grids, of which 25 are within the droplet, are sufficient to resolve the flowfield in the present work.

In the numerical simulations, the droplet vaporization process is terminated when the mass fraction ratio,  $(Y_{O_2, \text{int}} - Y_{O_2, \text{bub}})/Y_{O_2, \text{int}}$ , drops below 2%, which is defined as the saturation condition, or when the temperature difference between the bubble and droplet surface is less than 5 K. These

conditions can be met with a highly dense droplet cluster, leading to a very small droplet bubble. The variables,  $Y_{O_2, \text{int}}$  and  $Y_{O_2, \text{bub}}$ , represent the mass fractions of oxygen at the droplet and bubble surfaces, respectively. Under the saturation condition, a droplet vaporization process terminates due to mass transfer limitations.

The effect of pressure on the clustered droplet vaporization behavior is first investigated. Fig. 2 shows results for two different ambient temperatures, 1000 and 1500 K. The dimensionless parameter  $\tau$  is defined as the ratio of the lifetime of a single isolated droplet to its counterpart in a cluster. The former is obtained when the ratio of the initial radius of the bubble to that of the droplet,  $(R_{\text{bub}}/R_{d0})$  (defined as the interactive radius ratio), is 100, at which point the droplet interactions are negligible. The ambient pressure exerts strong influence on droplet clustering behaviors. For a given  $(R_{\text{bub}}/R_{d0})$ ,  $\tau$  decreases with decreasing pressure, indicating a prolonged droplet lifetime in a bubble. At a high ambient

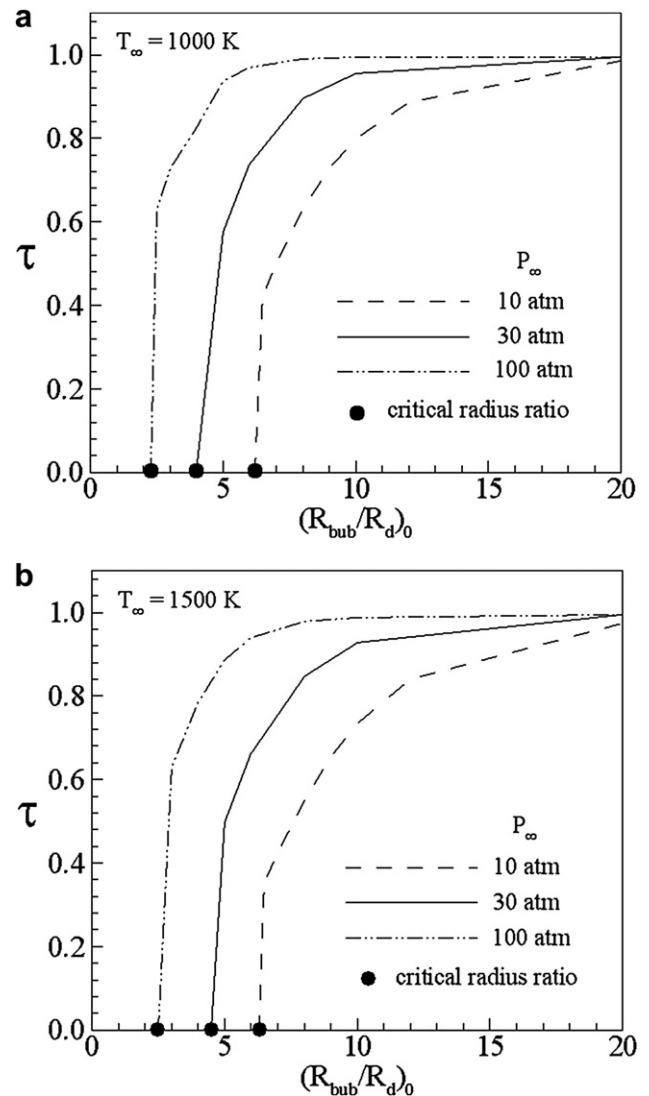


**Fig. 2 – Effect of ambient pressure on droplet lifetime as a function of the interactive radius ratio; (a) at 1000 K, and (b) at 1500 K.**

pressure, such as 100 atm, the droplet clustering effect becomes weak. In addition, the critical interactive radius ratio,  $(R_{bub}/R_d)_{0,crit}$ , at which complete droplet vaporization cannot be sustained, decreases significantly with increasing pressure. At both ambient temperatures, the critical radius ratios at 100 atm are around 2.5. They increase to a value larger than 6 at 10 atm.

Fig. 3 shows the effect of the ambient temperature on the clustered droplet vaporization behavior at two different ambient pressures, 30 and 100 atm, corresponding to the subcritical and supercritical conditions, respectively. The ambient temperature plays a much more minor role in determining the normalized droplet lifetime, compared with the pressure effect.

Droplet clustering behaviors are influenced mainly by two factors: heat and mass transfer rates at the droplet surface, which are dictated by gradients of the temperature and oxygen concentration on the gaseous side of the interface.

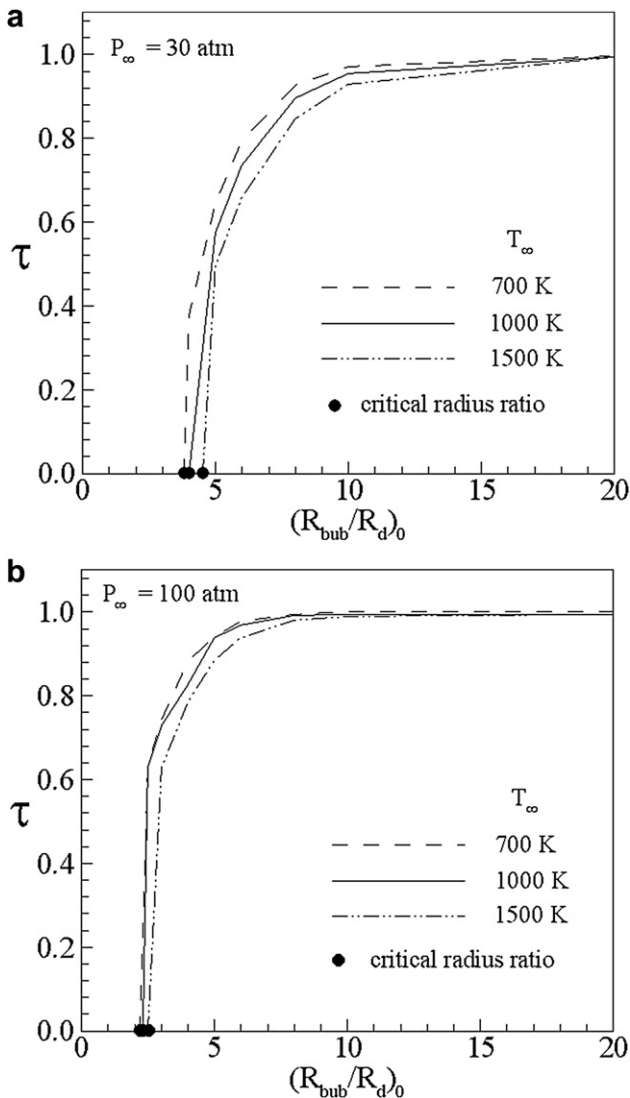


Fig. 3 – Effect of ambient temperature on droplet lifetime as a function of the interactive radius ratio; (a) at 30 atm, and (b) at 100 atm.

Fig. 4 shows the instantaneous temperature and oxygen mass-fraction distributions at an ambient pressure of 30 atm for a single droplet and a droplet in a dense cluster with  $(R_{bub}/R_d)_0 = 5$  at two different time instants corresponding to 20 and 80% of the droplet mass vaporization, respectively. The difference between the single droplet and the clustering case is small in the early stage of the droplet lifetime, when only 20% of the oxygen droplet is evaporated. The difference grows significantly when 80% of the oxygen mass is evaporated. The same trend is observed at a supercritical pressure of 100 atm, as shown in Fig. 5. These results clearly indicate that the decrease in heat and mass transfer rates at the droplet surface as the droplet evaporates result in droplet lifetime prolongation in a dense cluster environment.

Comparison of the results shown in Figs. 4 and 5 indicates that at a high ambient pressure, the differences in the temperature and mass fraction gradients between a single and a clustered droplet are much smaller in the late stages of the vaporization process in comparison with the situation at low pressure, mainly because more hydrogen mass and

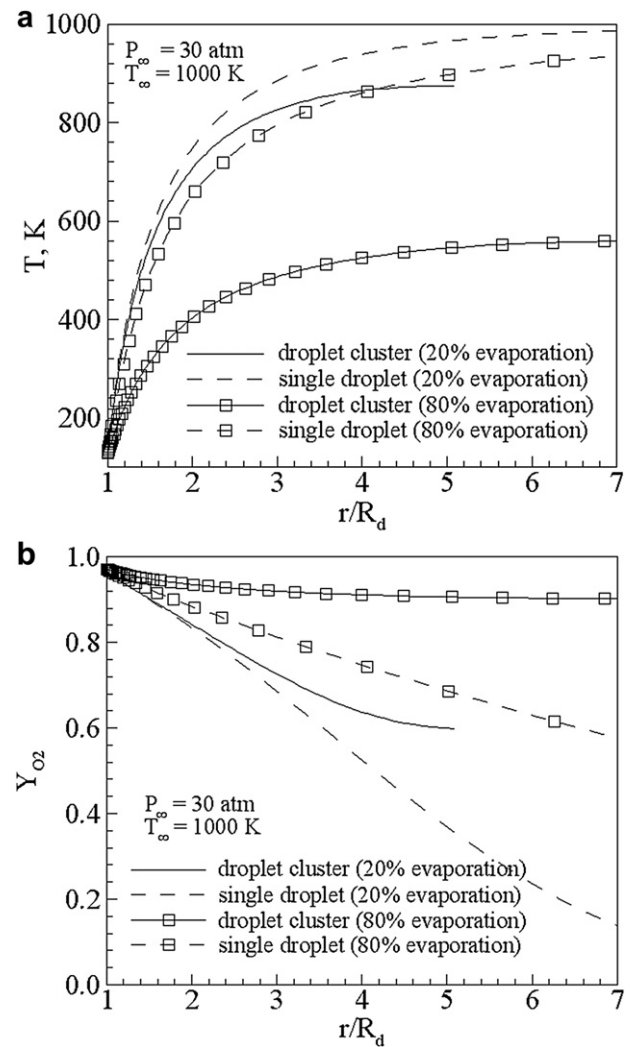
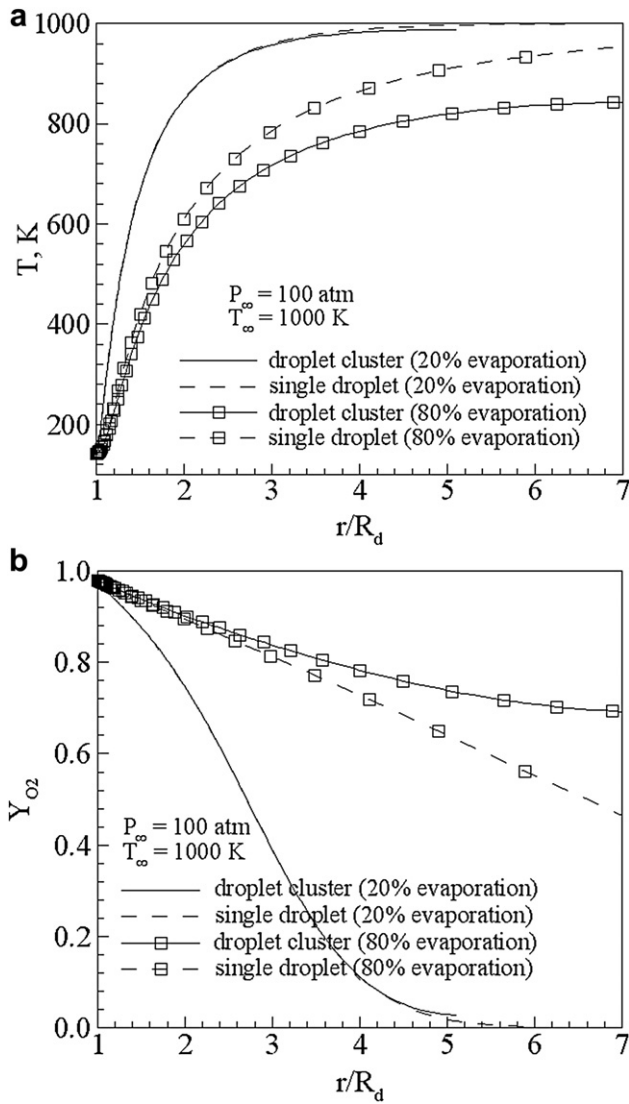


Fig. 4 – Instantaneous distributions of (a) temperature and (b) oxygen mass fraction at 30 atm and 1000 K at two time instants.



**Fig. 5 – Instantaneous distributions of (a) temperature and (b) oxygen mass fraction at 100 atm and 1000 K at two time instants.**

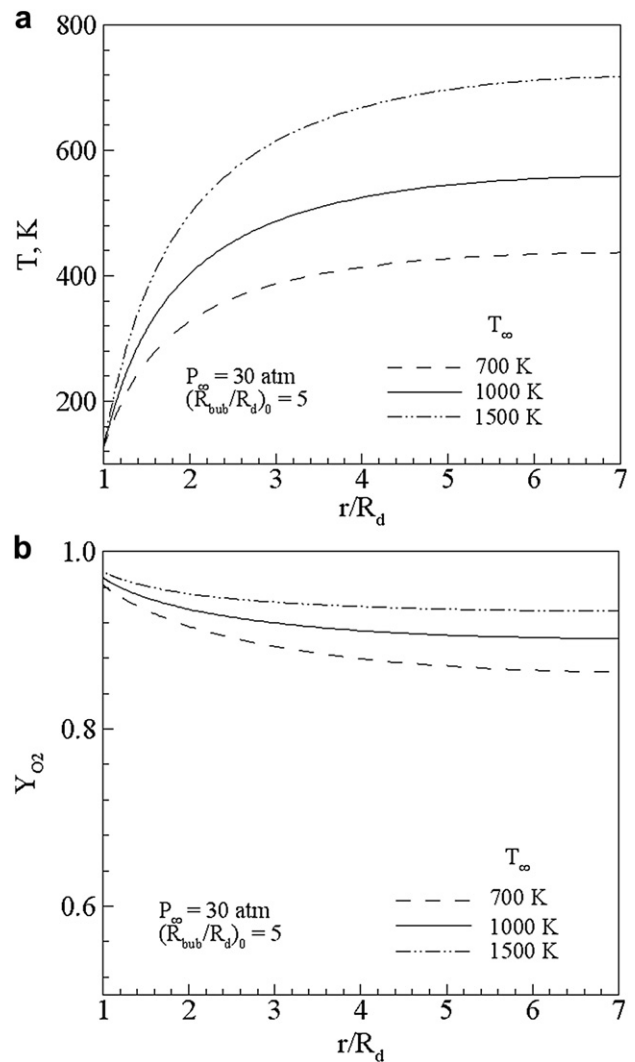
energy are initially stored in a fixed droplet bubble under high pressure. This phenomenon is consistent with the pressure effect on the dimensionless droplet lifetime shown in Fig. 2.

Fig. 6 shows the instantaneous distributions of the temperature and oxygen mass fraction outside the droplet when 80% of the liquid oxygen mass is evaporated. Three different ambient temperatures are considered under an ambient subcritical pressure of 30 atm. At a high ambient temperature, such as 1500 K, the temperature gradient at the droplet surface remains large even at the late stage of the droplet vaporization process. The mass fraction gradient, however, becomes low. Fig. 7 shows a similar phenomenon for the supercritical case at 100 atm. A higher ambient temperature enhances the heat transfer into the droplet, but hinders the oxygen mass transfer towards the surroundings. These two counteracting factors balance each other, resulting in

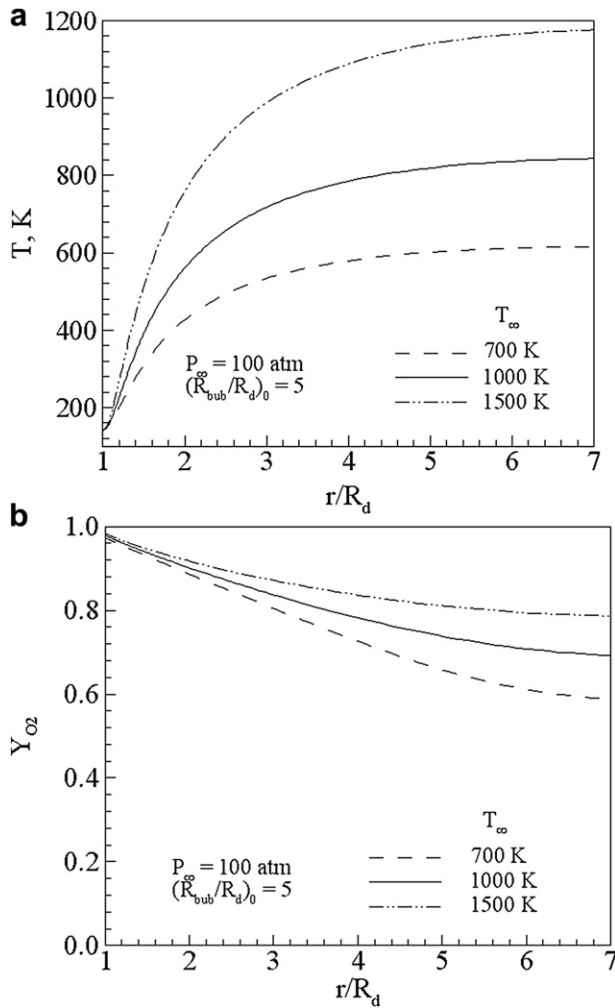
a weak temperature effect on the droplet clustering behavior, as evidenced in Fig. 3.

Fig. 8 shows the effect of the ambient pressure on the distributions of the temperature and oxygen mass fraction outside the droplet at the late stage of the droplet vaporization process, when 80% of the liquid oxygen mass is evaporated. The ambient temperature is 1000 K. In contrast to the results shown in Figs. 6 and 7, at a supercritical pressure of 100 atm, both the temperature and mass-fraction gradients at the droplet surface becomes much steeper, leading to both enhanced energy transfer into the droplet and increased mass transfer towards the surroundings. These two factors combined give rise to significant pressure effect on the droplet clustering behavior shown in Fig. 2.

As a droplet evaporates in an isolated gas bubble in a dense cluster, both the pressure and temperature effects on the heat and mass transfer rates are dictated by the initial gaseous mass and energy in the bubble. The initial mass of gaseous hydrogen depends mainly on its density, while the initial



**Fig. 6 – Effect of ambient temperature on the instantaneous distributions of (a) temperature and (b) oxygen mass fraction outside the droplet at 30 atm; 80% of droplet mass evaporated.**



**Fig. 7 – Effect of ambient temperature on the instantaneous distributions of (a) temperature and (b) oxygen mass fraction outside the droplet at 100 atm; 80% of droplet mass evaporated.**

energy in the bubble is determined by both the gaseous density and temperature. At a given bubble size and ambient temperature, when the ambient pressure is increased, the gaseous hydrogen density increases accordingly, as listed in Table 2. This results in more hydrogen mass surrounding the oxygen droplet and more energy for droplet vaporization. However, at a given bubble size and ambient pressure, increasing the initial ambient temperature leads to a decreased hydrogen density and thus less hydrogen mass. Table 3 lists the hydrogen density as a function of temperature. In this way, although the initial energy contained in the gas bubble is increased, leading to the enhanced heat transfer, the mass transfer is hindered at the late stage of the droplet vaporization process, as shown in Figs. 6 and 7.

Fig. 9 shows the clustering effects on the droplet vaporization rate at two different ambient pressures of 30 and 100 atm. The ambient temperature is fixed at 1000 K. The transient variations of the normalized droplet diameter squared,  $D^2/D_0^2$ , are presented. At a subcritical pressure of 30 atm, the droplet interaction is negligible when the interactive radius ratio exceeds 10. The clustering effects, however,

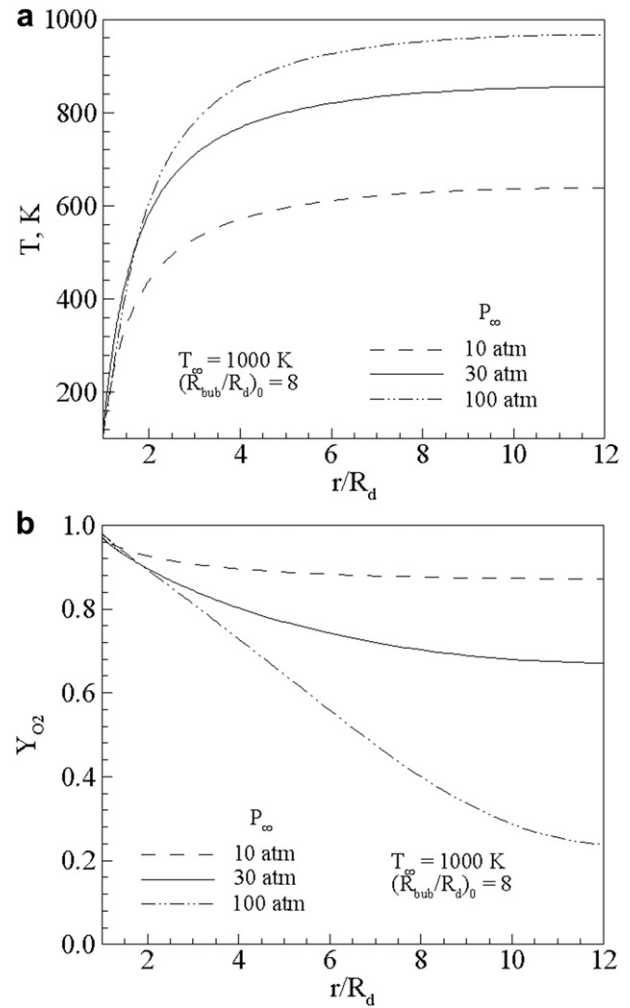


**Fig. 8 – Effect of ambient pressure on the instantaneous distributions of (a) temperature and (b) oxygen mass fraction outside the droplet at 1000 K; 80% of droplet mass evaporated.**

**Table 2 – Oxygen and hydrogen densities at various states.**

Pressure (atm)	Density of H <sub>2</sub> at 1000 K (kg/m <sup>3</sup> )	Density of O <sub>2</sub> at 100 K (kg/m <sup>3</sup> )
10	0.240	1087.2
30	0.717	1094.8
100	2.355	1118.0

**Table 3 – Effect of temperature on hydrogen density.**

Temperature (K)	Density of H <sub>2</sub> at 30 atm (kg/m <sup>3</sup> )
700	1.022
1000	0.717
1500	0.479

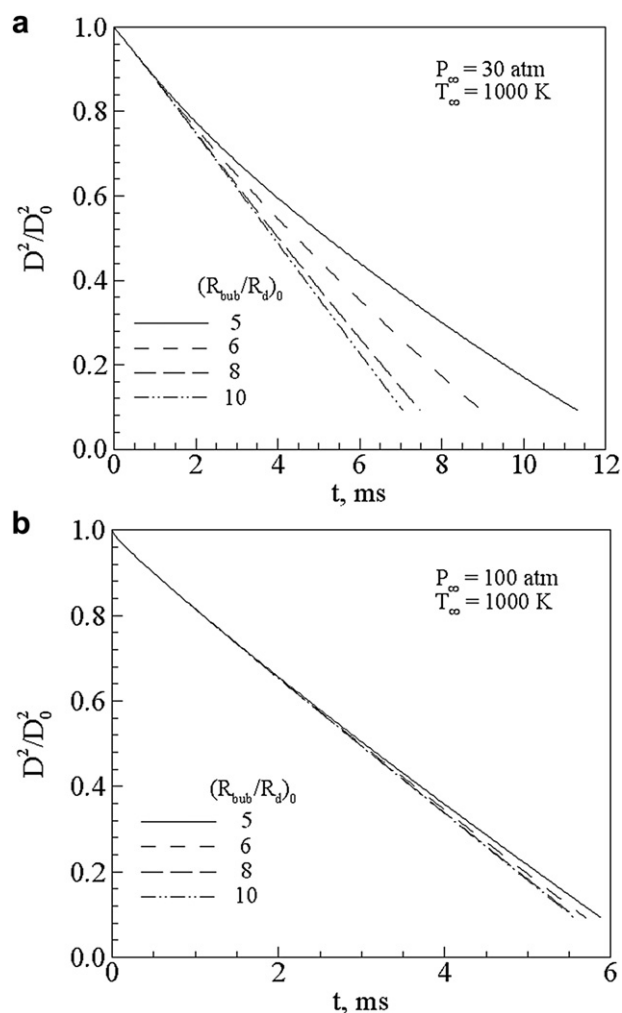


**Fig. 9 – Clustering effects on droplet vaporization rate at (a) 30 atm and (b) 100 atm.**

become significant when the droplets are highly packed. At an interactive radius ratio of 5, the droplet lifetime increases more than 60% compared with the situation with an isolated droplet.

At a supercritical pressure of 100 atm, as shown in Fig. 9b, the clustering effects on droplet vaporization become very weak. The droplet vaporization rate remains basically unchanged with the interactive radius ratio ranging from 5 to 10. This again confirms the results shown in Fig. 2 concerning the pressure effect on the droplet clustering behavior.

#### 4. Concluding remarks

In this paper, a droplet-in-bubble approach is incorporated into a previously developed and well-validated droplet vaporization model to study the clustering effects on droplet vaporization behaviors. The model accommodates all important high-pressure characteristics, including transient transport phenomena, dissolution of ambient gases into liquid droplets, thermodynamic non-idealities, and drastic variations of thermophysical properties. A liquid oxygen (LOX)

droplet evaporating in hydrogen environments under both sub- and supercritical conditions is treated. Special attention is given to the effects of ambient pressure and temperature on droplet vaporization in a dense cluster.

Results indicate that the ambient pressure exerts a strong influence on the droplet clustering behaviors. As pressure increases, the initial hydrogen mass and energy in a bubble inside a dense cluster environment increase significantly, leading to enhanced heat and mass transfer at the droplet surface. Droplet interactions are thus reduced, and the droplet vaporization time decreases.

The effect of the ambient temperature on droplet clustering behaviors appears to be weak. As temperature increases, the initial energy surrounding a droplet increases. The initial hydrogen mass in a bubble, however, decreases. The two effects combined lead to enhanced heat transfer but decreased mass transfer at the droplet surface. The process becomes even more evident at the late stage of the vaporization process. These two counteracting factors balance each other, producing weak temperature effects on droplet interactions.

#### Acknowledgement

HM would like to thank the Zhejiang Provincial Natural Science Foundation of China (R1100300) for financial support.

#### REFERENCES

- [1] Yang V. Modeling of supercritical vaporization, mixing, and combustion processes in liquid-fueled Propulsion Systems. *Proceeding of Combustion Institute* 2001;28:925–42.
- [2] Hsieh KC, Shuen JS, Yang V. Droplet vaporization in high-pressure environments I: near critical conditions. *Combustion Science and Technology* 1991;76:111–32.
- [3] Shuen JS, Yang V, Hsiao GC. Combustion of liquid-fuel droplets at supercritical conditions. *Combustion and Flame* 1992;89:299–319.
- [4] Delplanque JP, Sirignano WA. Numerical study of the transient vaporization of an oxygen droplet at sub- and super-critical conditions. *International Journal of Heat and Mass Transfer* 1993;36:303–14.
- [5] Yang V, Lin NN, Shuen JS. Vaporization of liquid oxygen (LOX) droplets in supercritical hydrogen environments. *Combustion Science and Technology* 1994;97:247–70.
- [6] Nomura H, Ujiie Y, Rath HJ, Sato J, Kono M. Experimental study on high pressure droplet evaporation using microgravity conditions. *Proceeding of Combustion Institute* 1996;26:1267–73.
- [7] Sirignano WA, Delplanque JP. Transcritical vaporization of liquid fuels and Propellants. *Journal of Propulsion and Power* 1999;15:896–902.
- [8] Chauveau C, Gökalp I, Segawa D, Kadota T, Enomoto H. Effects of reduced gravity on methanol droplet combustion at high pressures. *Proceedings of the Combustion Institute* 2001;28:1071–7.
- [9] Zhu GS, Reitz RD. A model for high-pressure vaporization of droplets of complex liquid mixtures using continuous thermodynamics. *International Journal of Heat and Mass Transfer* 2002;45:495–507.

- [10] Meng H, Hsiao GC, Yang V, Shuen JS. Transport and dynamics of liquid oxygen droplets in supercritical hydrogen streams. *Journal of Fluid Mechanics* 2005;527:115–39.
- [11] Yan C, Aggarwal SK. A high-pressure droplet model for spray simulations. *Journal of Engineering for Gas Turbine and Power* 2006;128:482–92.
- [12] Lafon P, Meng H, Yang V, Habiballah M. Vaporization of liquid oxygen (LOX) droplets in hydrogen and water environments under sub- and super-critical conditions. *Combustion Science and Technology* 2008;180:1–26.
- [13] Hsiao GC, Meng H, Yang V. Pressure-Coupled vaporization Response of n-pentane fuel droplet at subcritical and supercritical conditions. *Proceeding of Combustion Institute* 2011;33:1997–2003.
- [14] Chigier N. Optical imaging sprays. *Progress in Energy and Combustion Science* 1991;17:211–62.
- [15] Linne MA, Paciaroni M, Berrocal E, Sedarsky D. Ballistic Imaging of liquid Breakup processes in dense sprays. *Proceeding of Combustion Institute* 2009;32:2147–61.
- [16] Jiang TL, Chiang WT. Effects of multiple droplet interaction on droplet vaporization in subcritical and supercritical pressure environments. *Combustion and Flame* 1994;97:17–34.
- [17] Bellan J, Cuffel R. A theory of nondilute spray evaporation based upon multiple drop interaction. *Combustion and Flame* 1983;51:55–67.
- [18] Harstad K, Bellan J. Interactions of fluid oxygen drops in fluid hydrogen at rocket chamber pressures. *International Journal of Heat and Mass Transfer* 1998;41:3551–8.
- [19] Tishkoff JM. A model for the effect of droplet interactions on vaporization. *International Journal of Heat and Mass Transfer* 1979;22:1407–15.
- [20] Meng H, Yang V. A unified treatment of general fluid thermodynamics and its application to a preconditioning scheme. *Journal of Computational Physics* 2003;189:277–304.
- [21] Zong N, Meng H, Hiesh S-Y, Yang V. A numerical study of cryogenic fluid injection and mixing under supercritical conditions. *Physics of Fluids* 2004;16:4248–61.
- [22] Zong N, Yang V. Cryogenic fluid jets and mixing layers in transcritical and supercritical environments. *Combustion Science and Technology* 2006;178:193–227.
- [23] Zong N, Yang V. Near-Field flow and flame dynamics of LOX/Methane shear coaxial injector under supercritical conditions. *Proceedings of the Combustion Institute* 2007;31:2309–17.
- [24] Zong N, Yang V. Cryogenic fluid dynamics of pressure swirl injectors at supercritical conditions. *Physics of Fluids* 2008;20:056103.
- [25] Hua Y-X, Wang Y-Z, Meng H. A numerical study of supercritical forced convective heat transfer of n-heptane inside a horizontal miniature tube. *The Journal of Supercritical Fluids* 2010;52:36–46.
- [26] Wang Y-Z, Hua Y-X, Meng H. Numerical studies of supercritical turbulent convective heat transfer of cryogenic-Propellant Methane. *Journal of Thermophysics and Heat Transfer* 2010;24:490–500.
- [27] Ruan B, Meng H. Supercritical heat transfer of cryogenic-propellant methane in rectangular engine cooling channels. *Journal of Thermophysics and Heat Transfer* 2012;26:313–21.